Reactivity of a Titanium Dinitrogen Complex Supported by Guanidinate Ligands: Investigation of Solution Behavior and a Novel Rearrangement of Guanidinate Ligands

Sarah M. Mullins, Andrew P. Duncan, Robert G. Bergman,* and John Arnold*

Department of Chemistry and Center for New Directions in Organic Synthesis (CNDOS), University of California and Division of Chemical Sciences, Lawrence Berkeley National Laboratory, Berkeley, California 94720-1460

Received June 14, 2001

The titanium dinitrogen complex, $\{[(Me_2N)C(N^iPr)_2]_2Ti\}_2(N_2)$ (**2**), was synthesized by reduction of the dichloride precursor, $[(Me_2N)C(N^iPr)_2]_2TiCl_2$ (**1**). The dinitrogen complex reacts with phenyl azide to yield the titanium imido complex, $[(Me_2N)C(N^iPr)_2]_2TiNPh$ (**3**). The fluxional behavior of the guanidinate ligands in compounds **1**−**3** was investigated using variable temperature and two-dimensional NMR techniques; guanidinate ligand rotation and racemization reactions were observed. Rearrangement of the guanidinate ligand to an asymmetrical bonding mode utilizing the dimethylamino and amide-nitrogen atoms is observed in the bridging oxo and sulfido derivatives (**4** and **5**). These compounds are formed by the reactions of **2** with pyridine *N*-oxide and propylene sulfide, respectively. The ligand rearrangement was observed to be reversible for the bridging sulfido complex **5**; the structure of this compound is sensitive to temperature and solvent. The solid-state and solution structures of compounds **1**−**5** are discussed.

Introduction

The development of new ancillary ligands has been vital to the discovery of new metal-mediated organic transformations. Of particular interest has been the exploration of support ligands in which hard base donors are coordinated to metals so as to enforce a cis arrangement of the reactive ligands. To this end, a variety of new multidentate anionic ligands bearing nitrogen donor atoms, including diamido,[1−3] β-diketiminate,[4] aminotroponiminate,[5,6] amidinate,[7−11] and guanidinate ligands have been studied. We have been interested in guanidinate ligands because of their potential for steric and electronic tunability.

Guanidinate anions are closely related to amidinates, differing only in that they contain an amino (R_2N) substituent on the ligand's central carbon. In one of the two resonance structures of an η^2-guanidinate−metal interaction, lone pair donation from the R_2N group places a formal negative charge on the metal center (structure **B** in Figure 1). We propose that donation from the dialkylamino lone pair into the chelate may provide a ligand that, while formally isoelectronic to an amidinate, will render its metal complexes more electron rich. However, the electronic properties of other metal-bound ligands (e.g., chloride, alkyl, imido, oxo, sulfido) may also influence the bonding structure of the guanidinate. Jordan and co-workers have proposed that steric repulsion between the alkyl substituents on the noncoordinated amino group and the substituents on the chelating nitrogen atoms disfavors resonance structure **B** in aluminum guanidinate complexes.[12]

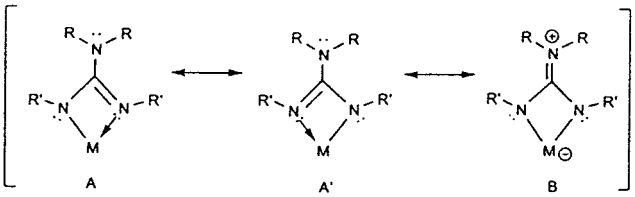

Figure 1. Resonance structures for the metal-bound guanidinate ligand.

The first transition metal guanidinate complexes, reported by Lappert et al. in 1970, were generated by formal insertion of carbodiimides into homoleptic titanium and zirconium amides.[13] This approach has recently been extended to other early metals.[14] Neutral guanidines and lithium guanidinates have been utilized for the synthesis of late metal,[15−17] early metal,[18−20] and f block compounds,[18,21] and several research groups have investigated the structural parameters of the guanidinate ligands in these

* To whom correspondence should be addressed.

(1) Kempe, R. *Angew. Chem., Intl. Ed.* **2000**, *39*, 468.
(2) Baumann, R.; Stumpf, R.; Davis, W. M.; Liang, L.-C.; Schrock, R. R. *J. Am. Chem. Soc.* **1999**, *121*, 7822.
(3) Gade, L. *J. Chem. Soc., Chem. Commun.* **2000**, 173−181.
(4) Kakaliou, L.; Scanlon, W. J.; Qian, B.; Baek, S. W.; Smith, M. R.; Motry, D. H. *Inorg. Chem.* **1999**, *38*, 5964.
(5) Steinhuebel, D. P.; Lippard, S. J. *Organometallics* **1999**, *18*, 109.
(6) Roesky, P. W. *Chem. Soc. Rev.* **2000**, *29*, 335.
(7) Hagadorn, J. R.; Arnold, J. *Inorg. Chem.* **1997**, *36*, 2928.
(8) Hagadorn, J. R.; Arnold, J. *J. Am. Chem. Soc.* **1996**, *118*, 893.
(9) Roesky, H. W.; Meller, B.; Noltemeyer, M.; Schmidt, H. G.; Scholz, U.; Sheldrick, G. M. *Chem. Ber.* **1988**, *121*, 1403.
(10) Stewart, P. J.; Blake, A. J.; Mountford, P. *Inorg. Chem.* **1997**, *36*, 3616.
(11) Kempe, R.; Arndt, P. *Inorg. Chem.* **1996**, *35*, 2644.
(12) Aeilts, S. L.; Coles, M. P.; Swenson, D. C.; Jordan, R. F. *Organometallics* **1998**, *17*, 3265.
(13) Chandra, G.; Jenkins, A. D.; Lappert, M. F.; Srivastava, R. C. *J. Chem. Soc. A* **1970**, 2550.
(14) Tin, M. K. T.; Yap, G. P. A.; Richeson, D. S. *Inorg. Chem.* **1999**, *38*, 998.
(15) Bailey, P. J.; Mitchell, L. A.; Parsons, S. *J. Chem. Soc., Dalton Trans.* **1996**, 2839.
(16) Robinson, S. D.; Sahajpal, A. *J. Chem. Soc., Dalton Trans.* **1997**, 3349.
(17) Holman, K. T.; Robinson, S. D.; Sahajpal, A.; Steed, J. W. *J. Chem. Soc., Dalton Trans.* **1999**, 15.
(18) Giesbrecht, G. R.; Arnold, J. *J. Chem. Soc., Dalton Trans.* **2001**, in press.
(19) Wood, D.; Yap, G. P. A.; Richeson, D. S. *Inorg. Chem.* **1999**, *38*, 5788.
(20) Duncan, A. P.; Mullins, S. M.; Arnold, J.; Bergman, R. G. *Organometallics* **2001**, *20*, 1808.

10.1021/ic010631+ CCC: $20.00
Published on Web 11/22/2001

complexes.[15,19,20,22] Whereas guanidinate ligands have been utilized to support a variety of transition metals,[23] there is surprisingly little chemistry reported for titanium.[13,22]

We considered that the bis(guanidinate) ligand set would be appropriate for the study of heteroatom (O, S, NR) abstraction reactions with d^2 titanium complexes. The guanidinate ligands on the reduced metal atom should produce an electron-rich, and consequently easily oxidized, titanium center. This electronic effect may also increase the nucleophilicity of d^0 M = X (X = O, S, NR) metal−ligand multiply bonded complexes. The substituents on the $[Me_2NC(N^iPr)_2]^-$ guanidinate ligand were chosen to maximize electron donation from the dialkyl amino group.

Herein, we report the synthesis of a dimeric bis(guanidinate) titanium dinitrogen complex and its behavior in heteroatom (O, S, NR) transfer reactions. Analysis of the X-ray structures, with particular attention to the guanidinate bonding, is discussed. The solution behavior of the complexes, including fluxionality within and isomerization of the metal complexes and a novel guanidinate rearrangement, is also described.

Results and Discussion

Chloro and Alkyl Derivatives. The dichloride complex $[Me_2NC(N^iPr)_2]_2TiCl_2$ (**1**) was synthesized in >90% yield by addition of 2 equiv of ^{i}PrNCN^{i}Pr to $(Me_2N)_2TiCl_2$ in diethyl ether solution (eq 1).

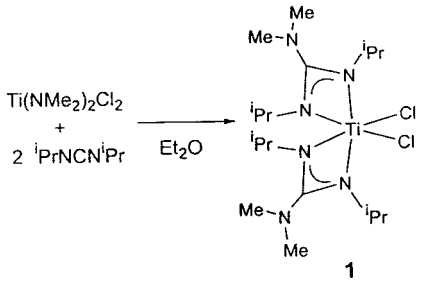

(1)

1

Complex **1** can also be synthesized by salt metathesis between $TiCl_4(THF)_2$ and 2 equiv of the lithium guanidinate (generated in situ from $LiNMe_2$ and ^{i}PrNCN^{i}Pr) in ether, but lower yields are obtained with this method.

The room temperature ^{1}H NMR spectrum of **1** in C_6D_6 shows one set of broad resonances for the isopropyl groups, indicating fluxional behavior of the complex. At the slow exchange limit (−55 °C in toluene-d_8), the aliphatic region of the spectrum sharpens to four doublets and two septets, corresponding to the methyl (**a**, **b**, **d**, **e**) and the methine (**c**, **f**) resonances of the isopropyl group, respectively (Figure 2).[24] Fast exchange is observed upon heating **1** to 70 °C; at this temperature, one septet and one doublet are observed for the isopropyl methine and methyl resonances, respectively. A single resonance for the dimethylamino groups is observed at all temperatures.

Two-dimensional NMR experiments were used to elucidate the fluxional behavior within each guanidinate ligand. A ^{1}H−^{1}H TOCSY experiment (Figure 3) was performed at the slow exchange limit (−53 °C), and this spectrum was used to assign the connectivity of the isopropyl groups. Resonances **a** and **b** are coupled to each other and to resonance **c**; resonances **d** and **e** are coupled to each other and to resonance **f**. A ^{1}H−^{1}H NOESY experiment at −31 °C (Figure 4) revealed exchange cross peaks between all four methyl group protons (**a**, **b**, **d**, **e** in Figure 2); exchange cross peaks were also observed between the two methine protons (**c**, **f**).

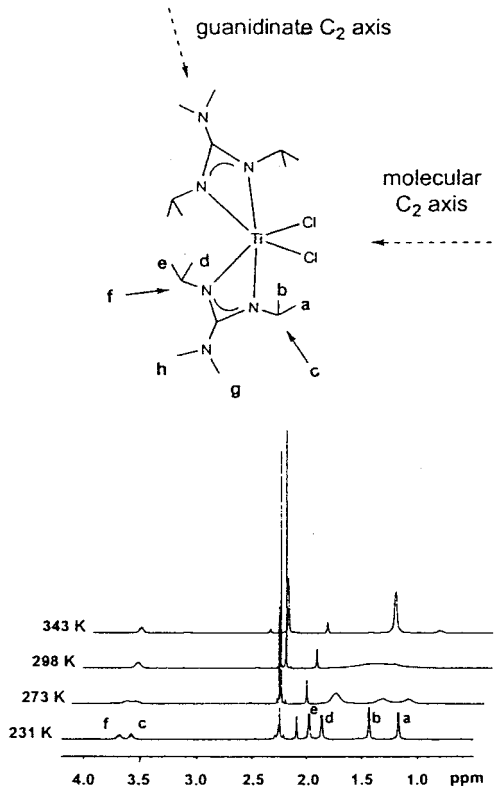

Figure 2. Assignment of proton resonances in **1** in toluene-d_8 at the slow exchange limit; relation of the isopropyl methyls of the two guanidinates.

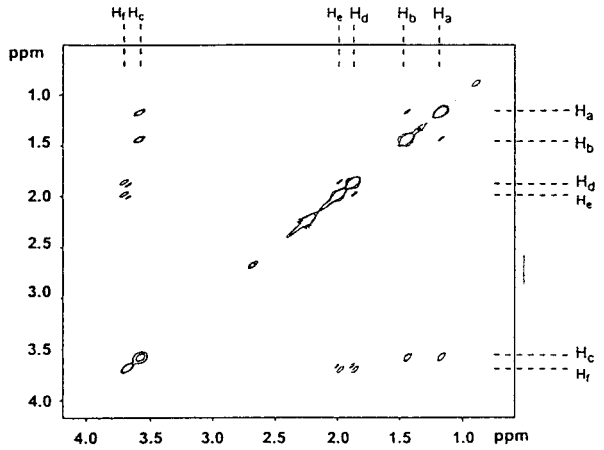

Figure 3. ^{1}H−^{1}H TOCSY spectrum at −53 °C (toluene-d_8).

The observation that the eight isopropyl methyl groups of **1** give rise to only four doublets at low temperature and one doublet at high temperature is explained by the C_2 symmetry of the molecule in solution (Figure 2). Due to this symmetry, the two guanidinate ligands are magnetically equivalent at all temperatures. At high temperature, racemization of **1** combined with rotation of the guanidinate ligand about its internal C_2 axis[25]

(21) Zhou, Y.; Yap, G. P. A.; Richeson, D. S. *Organometallics* **1998**, *17*, 4387.
(22) Bailey, P. J.; Grant, K. J.; Mitchell, L. A.; Pace, S.; Parkin, A.; Parsons, S. *J. Chem. Soc., Dalton Trans.* **2000**, 1887.
(23) Bailey, P. J.; Pace, S. *Coord. Chem. Rev.* **2001**, *214*, 91.
(24) Since there is no way to render an absolute assignment within the category of proton type (methyl-**a**, **b**, **d**, **e** or methine-**c**, **f**), assignments are arbitrary within these categories and for labeling convenience only.
(25) Rotation around the internal C_2 axis has been observed in amidinate complexes. See: Koterwas, L. A., Fettinger, J. C., Sita, L. R. *Organometallics*, **1999**, *18*, 4183.

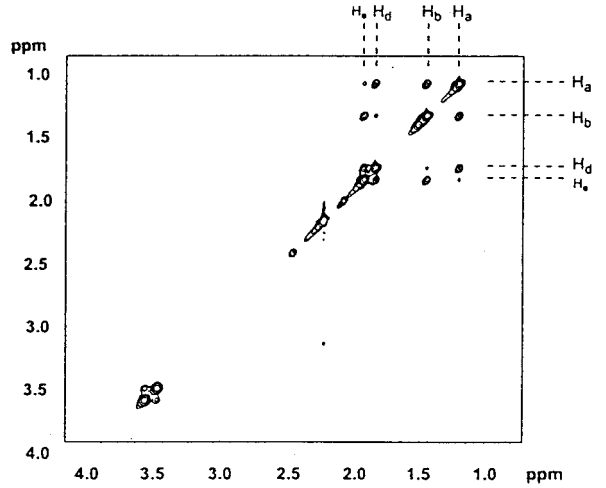

Figure 4. $^1H-^1H$ NOESY spectrum at −31 °C (toluene-d_8).

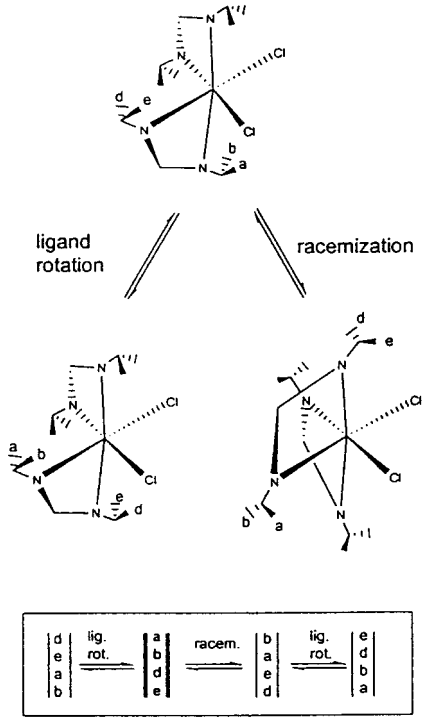

Figure 5. Guanidinate ligand rotation and racemization processes of the metal complexes.

equilibrates the four isopropyl methyl groups of a given guanidinate ligand (**a**, **b**, **d**, **e**) (Figure 5); consequently, one resonance is observed for these protons. Several intramolecular racemization mechanisms are possible, including trigonal twist, rhombic twist, and ring-opening pathways.[26−28] At low temperature, both exchange processes are slowed sufficiently so that the proton resonances of the diastereotopic methyls appear as four distinct resonances.

The C_2 symmetry observed in solution is consistent with the solid-state structure of complex **1**. X-ray quality crystals of **1** were grown from pentane solution at −30 °C. The ORTEP diagram is shown in Figure 6. Bond lengths and angles are given

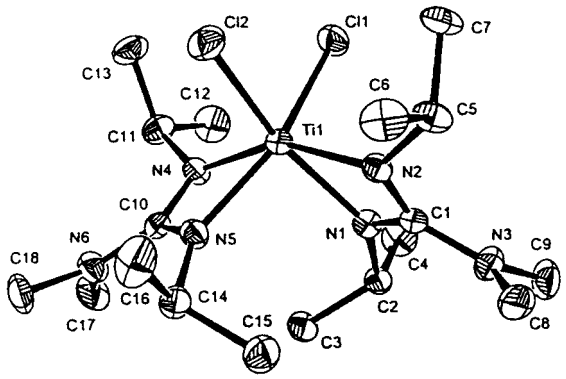

Figure 6. ORTEP diagram of **1**, showing 50% thermal probability ellipsoids. Hydrogen atoms are omitted for clarity.

Table 1. Selected Bond Lengths (Å) and Angles (deg) for **1**

Ti(1)	Cl(1)		2.3261(7)	Ti(1)	Cl(2)		2.3302(7)
Ti(1)	N(1)		2.093(2)	Ti(1)	N(2)		2.049(2)
Ti(1)	N(4)		2.058(2)	Ti(1)	N(5)		2.061(2)
Cl(1)	Ti(1)	N(2)	102.47(5)	Cl(1)	Ti(1)	N(1)	93.16(5)
Cl(1)	Ti(1)	N(5)	157.21(5)	Cl(1)	Ti(1)	N(4)	93.29(5)
Cl(2)	Ti(1)	N(2)	94.71(5)	Cl(2)	Ti(1)	N(1)	158.61(5)
Cl(2)	Ti(1)	N(5)	90.64(5)	Cl(2)	Ti(1)	N(4)	104.67(5)
N(1)	Ti(1)	N(4)	95.90(7)	N(1)	Ti(1)	N(2)	63.90(7)
N(2)	Ti(1)	N(4)	154.68(7)	N(1)	Ti(1)	N(5)	93.08(7)
N(4)	Ti(1)	N(5)	64.27(7)	N(2)	Ti(1)	N(5)	99.96(7)
N(4)	C(10)	N(5)	109.0(2)	N(1)	C(1)	N(2)	109.0(2)
Cl(1)	Ti(1)	Cl(2)	91.49(2)				

in Table 1; selected crystal and refinement data are given in Table 2. A comparison of the metrical parameters of the guanidinate ligands in **1** and in the other titanium−guanidinate complexes will be discussed later.

Reduction of 1. Dichloride compound **1** reacts with Mg powder in THF under an atmosphere of nitrogen to yield the dinitrogen-bridged dimer, $\{[Me_2NC(N^iPr)_2]_2Ti\}_2(N_2)$ (**2**) (eq 2). Although ^1H NMR analysis of the crude reaction mixture shows

$$\mathbf{1} \xrightarrow[\text{THF}]{\text{xs Mg}^0,\ N_2} 0.5\ \underset{\mathbf{2}}{\{[Me_2NC(N^iPr)_2]_2Ti\}_2(N_2)} \qquad (2)$$

a single guanidinate-containing product, crystallization is required to separate **2** from the $MgCl_2$. The high solubility of **2** in hydrocarbon solvents leads to a purified yield of approximately 60%.

The variable temperature ^1H NMR spectra of **2** in C_6D_6 or toluene-d_8 reveal ligand exchange behavior analogous to that described for complex **1** (see above). However, ^1H NMR spectra of the dimer **2** are complicated by the presence of three stereoisomers (ΔΔ, ΛΛ, ΛΔ) in solution (Figure 7). Upon cooling to the slow exchange limit (−60 °C), a total of eight doublet resonances appear for the isopropyl methyl groups. Since the enantiomers (ΔΔ, ΛΛ) have D_2 symmetry, all four guanidinate ligands are magnetically equivalent and, therefore, give rise to four isopropyl methyl group resonances (**a**, **b**, **d**, **e**). Similarly, due to its C_{2h} symmetry, all four guanidinates of the meso (ΛΔ) compound are chemically equivalent; again, four isopropyl methyl group resonances (**g**, **h**, **j**, **k**) are observed. At high temperatures, one averaged doublet resonance is observed for the isopropyl groups of all three stereoisomers. The interconversion of the three stereoisomers combined with the rotation of the guanidinate ligands around their internal C_2 axes explains this behavior at the fast exchange limit.

Complex **2** crystallizes in the centrosymmetric space group *Pbcn* with a crystallographic two-fold axis present along the

(26) Cotton, F. A.; Wilkinson, G.; Murillo, C. A.; Bochmann, M. In *Advanced Inorganic Chemistry*; 6th ed.; John Wiley and Sons: New York, 1999; p 18.
(27) Banerjea, D.; Bailar, J. C. *Transition Met. Chem.* **1985**, *10*, 331.
(28) Palazzotto, M. C.; Duffy, D. J.; Edgar, B. L.; Que, L., Jr.; Pignolet, L. H. *J. Am. Chem. Soc.* **1973**, *95*, 4537.

Table 2. Crystallographic Data and Refinement Details for **1**−**3**

	1	**2**	**3**
empirical formula	$C_{18}N_6H_{40}Cl_2Ti$	$C_{36}H_{80}N_8Ti_2$	$C_{24}H_{45}N_7Ti$
formula weight	459.36	804.54	479.57
temp (°C)	−128	−100	−123
cryst syst	monoclinic	orthorhombic	orthorhombic
space group	$P2_1/n$ (#14)	*Pbcn* (#60)	*Pnna* (#52)
a (Å)	9.03670(10)	11.7853(2)	21.9307(7)
b (Å)	16.5529(4)	23.9649(6)	10.9904(3)
c (Å)	16.6918(4)	17.3657(2)	11.5032(4)
V (Å^3)	2418.30(8)	4904.7(1)	2772.6(1)
β (deg)	104.407(1)	90	90
Z	4	8	4
d_{calc} (g/cm^3)	1.262	1.464	1.149
diffractometer	Siemens SMART	Siemens SMART	Siemens SMART
radiation	Mo Kα	Mo Kα	Mo Kα
monochromator	graphite	graphite	graphite
detector	CCD area	CCD area	CCD area
scan type, deg	ω, 0.3	ω, 0.3	ω, 0.3
frame collection time (s)	10	10	10
reflns measured	hemisphere	hemisphere	hemisphere
2θ range (deg)	3−52.1	3−52.0	3−52.1
μ (mm^{-1})	5.90	5.07	3.32
T_{max}, T_{min}	0.831, 0.694	0.856, 0.620	0.931, 0.864
cryst dimensions (mm)	0.50 × 0.20 × 0.28	0.30 × 0.30 × 0.25	0.50 × 0.20 × 0.28
no. reflns measured	11704	23779	13414
no. unique reflns	4464	5029	2919
no. observations ($I > 3\sigma$)	3037	1905	1683
no. variables	244	235	147
data/parameter	12.45	8.11	11.45
refinement method	full-matrix least-squares on F^2	full-matrix least-squares on F^2	full-matrix least-squares on F^2
*R*int (%)	2.6	5.1	3.9
R (%)	2.7	4.9	3
*R*w (%)	3.3	6.3	3.9
GOF	1.2	2.17	1.32
largest diff. peak and hole e Å^{-3}	0.22 −0.27	0.44 −0.30	0.19 −0.21
hydrogen atoms	idealized positions	idealized positions	idealized positions

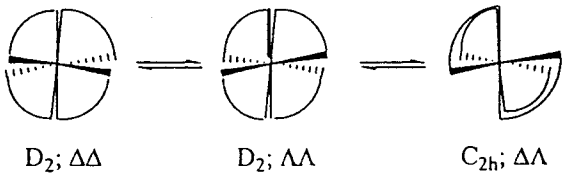

Figure 7. Interconversion of stereoisomers of **2**; the view is down the Ti−N−N−Ti vector.

Ti1−N7−N8−Ti2 vector. The ORTEP diagram is shown in Figure 8. Bond lengths and angles are given in Table 3; selected crystal and refinement data are given in Table 2. The Ti1−N7 and Ti2−N8 bond lengths (1.75(1) and 1.72(1) Å, respectively) are similar to known titanium nitrogen double bond distances.[29,30] However, the distance between N7 and N8 is only 1.28(1) Å; this is significantly longer than the triple bond of free dinitrogen (1.0975 Å),[31] but too short to be characterized as a single bond.[32] The bonding in **2** is best described as delocalized across the four bridging atoms, with partial double bond character in the N−N bond.[33]

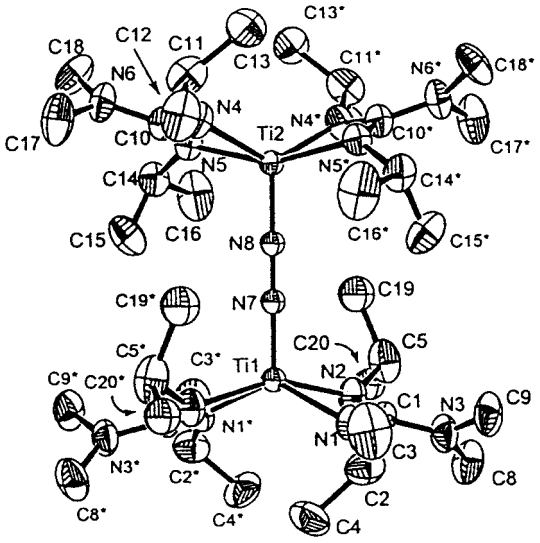

Figure 8. ORTEP diagram of **2**, showing 50% thermal probability ellipsoids. Hydrogens, C6/C6*, and C7/C7* (disordered isopropyl group) are omitted for clarity.

A comparison of these structural parameters with those of other known titanium complexes with end-on bridging dinitrogen ligands revealed several trends. The titanocene-based complexes $[Cp^*_2Ti]_2(N_2)$[34] and $[(C_5HMe_4)_2Ti]_2(N_2)$[35] have relatively short N−N bond lengths of 1.165[36] and 1.170(4) Å,[35] respectively (and long Ti−N bonds). These compounds and the

(29) Blake, A. J.; Collier, P. E.; Gade, L. H.; McPartlin, M.; Mountford, P.; Schubart, M.; Scowen, I. J. *J. Chem. Soc., Chem. Commun.* **1997**, 1555.
(30) Bai, Y.; Notlemeyer, M.; Roesky, H. W. *Z. Naturforsch. B* **1991**, *46b*, 1357.
(31) Wilkinson, P. G.; Houk, N. B. *J. Chem. Phys.* **1956**, *24*, 528.
(32) The N−N bond length of hydrazine is 1.46 Å; however, longer N−N bonds have been reported in transition metal complexes, see: Fryzuk, M. D., Love, J. B., Rettig, S. J., Young, V. G. *Science*, **1997**, *275*, 1445.
(33) Fryzuk, M. D.; Johnson, S. A. *Coord. Chem. Rev.* **2000**, *200*−*202*, 379.
(34) Bercaw, J. E.; Marvich, R. H.; Bell, L. G.; Brintzinger, H. H. *J. Am. Chem. Soc.* **1972**, *94*, 1219.

Table 3. Selected Bond Lengths (Å) and Angles (deg) for **2**

Ti(1)	N(1)	2.109(5)		Ti(1)	N(1)	2.109(5)	
Ti(1)	N(2)	2.141(4)		Ti(1)	N(2)	2.141(4)	
Ti(1)	N(7)	1.723(8)		Ti(2)	N(8)	1.744(8)	
Ti(2)	N(4)	2.114(5)		Ti(2)	N(5)	2.138(4)	
N(1)	Ti(1)	N(2)	63.2(2)	N(1)	Ti(1)	N(7)	114.2(1)
N(2)	Ti(1)	N(7)	102.8(1)	N(4)	Ti(2)	N(5)	63.3(2)
N(4)	Ti(2)	N(8)	115.7(1)	N(5)	Ti(2)	N(8)	102.6(1)

related, but not crystallographically characterized, $[Cp_2Ti]_2(N_2)$ complex[34] all release N_2 under reduced pressure. In contrast, the μ-N_2 complexes supported by nitrogen-based ancillary ligands all exhibit longer N−N bonds, e.g., $\{[PhC(NSiMe_3)_2]_2Ti\}_2(N_2)$ (N−N = 1.275(6) Å),[8] $[((Me_3Si)_2N)TiCl(TMEDA)]_2(N_2)$ (N−N = 1.289(9) Å),[37] and $[((Me_3Si)_2N)TiCl(py)_2]_2(N_2)$ (N−N = 1.263(7) Å).[38] These compounds all contain titanium centers with basically square pyramidal coordination environments. None of these compounds releases dinitrogen under reduced pressure. Compound **2** is similar to other μ-N_2 complexes supported by nitrogen-based ancillary ligands, in that its dinitrogen ligand is significantly more reduced than in metallocene analogues and is stable to reduced pressure.

Formation of Base Adducts. The structurally related μ-N_2 bis(benzamidinate) complex, $\{[PhC(NSiMe_3)_2]_2Ti\}_2(N_2)$,[8] forms isolable Lewis base adducts with pyridine and 2,6-xylylisocyanide. Addition of excess pyridine to a sample of **2** in C_6D_6 resulted in broadening of the pyridine resonances, suggesting reversible formation of a pyridine−titanium adduct. However, attempts to isolate this product resulted only in recovery of the starting material. The solution IR spectrum (C_6D_6) of a mixture of **2** with 2,6-xylylisocyanide revealed no change in the isocyanide CN stretch. While the resistance of **2** to coordination of Lewis bases is consistent with the titanium center of the bis(guanidinate) complex being more electron rich than the related amidinate complex, the steric differences between the guanidinate and amidinate ligands may also play a role in this reactivity. Attempts to isolate a guanidinate−titanium(II) complex with π backbonding ligands for comparison of IR stretches were unsuccessful.

Synthesis of Phenylimido Complex (3) from 1. Treatment of the dinitrogen complex **2** with 2 equiv of phenyl azide yielded the phenylimido complex $[Me_2NC(N^iPr)_2]_2Ti{=}NPh$ (**3**) (eq 3). The ^1H NMR spectrum of **3** in C_6D_6 shows sharp isopropyl

$$2 \xrightarrow[Et_2O]{2\ PhN_3} [(Me_2N)C(N^iPr)_2]_2TiNPh \quad (3)$$

3

group resonances at room temperature, but upon cooling to −66 °C, the spectrum resembles that of **1** at the slow exchange limit, except that the *N*-methyl resonances also decoalesce to two singlets. Assignment of the isopropyl methyl groups was made using the spectrum from a $^1H-^1H$ TOCSY experiment, as was done for **1**. Exchange behavior analogous to **1** was observed in a $^1H-^1H$ NOESY experiment.

X-ray quality crystals of **3** were grown from diethyl ether solution at low temperature. The ORTEP diagram is shown in

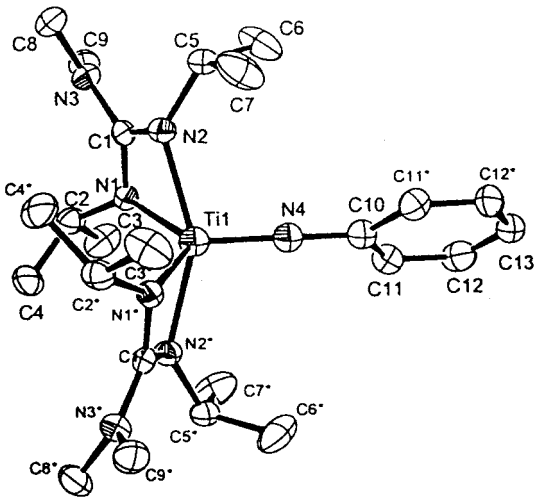

Figure 9. ORTEP diagram of **3**, showing 50% thermal probability ellipsoids. Hydrogen atoms are omitted for clarity.

Table 4. Selected Bond Lengths (Å) and Angles (deg) for **3**

Ti(1)	N(1)	2.108(2)		Ti(1)	N(2)	2.105(2)	
Ti(1)	N(4)	1.729(2)					
N(1)	Ti(1)	N(2)	63.97(6)	N(1)	Ti(1)	N(4)	119.31(5)
N(2)	Ti(1)	N(4)	104.53(5)	N(1)	C(1)	N(2)	112.1(2)

Figure 9. Bond lengths and angles are given in Table 4; selected crystal and refinement data are given in Table 2. The complex displays a distorted square pyramidal geometry, and a crystallographic C_2 axis lies along the Ti=NPh vector. The distance between Ti1 and N4 is 1.729(2) Å, which is similar to Ti=N bond distances in other imido complexes with N-based ancillary ligands.[29,39]

Synthesis of Oxo and Sulfido Derivatives. Ligand Rearrangement. Treatment of **2** with 2 equiv of pyridine *N*-oxide in toluene at −65 °C resulted in rapid formation of the dimeric bis(μ-oxo) complex **4** (eq 4).

$$2 \xrightarrow[\text{Toluene}]{2\ \text{O=N(C}_5\text{H}_5\text{)},\ -65\ ^\circ\text{C}} \{[Me_2NC(N^iPr)_2]_2TiO\}_2 \quad (4)$$

4

After crystallization from diethyl ether at low temperature, purified **4** was isolated in 71% yield. The X-ray crystal structure of **4** reveals that one guanidinate ligand on each titanium atom has undergone a rearrangement to a novel asymmetric coordination mode. The ORTEP diagram is shown in Figure 10. Bond lengths and angles are given in Table 5; selected crystal and refinement data are given in Table 6. The rearranged guanidinate ligands are bound through the amide nitrogen atoms (N4 and N10) and the dimethylamino nitrogen atoms (N5 and N11). The asymmetrically bound ligands are on the same side of the plane defined by the Ti_2O_2 core. The ring is planar (twist angle O1−Ti1−O2/O1−Ti2−O2, 176.33°) with inequivalent titanium−oxygen bond lengths. The Ti−O bonds trans to the dimethylamino nitrogen donors are shorter (Ti1−O1, 1.760(3) Å, trans to N5; Ti2−O2, 1.769(2) Å, trans to N11) than those trans to the amide donors (Ti1−O2, 1.915(3) Å; Ti2−O1, 1.932(3) Å), possibly due to the greater trans effect of the anionic nitrogens.

Whereas the symmetrically bound guanidinates of **4** exhibit delocalized bonding throughout the N_3C ligand core (see below),

(35) de Wolf, J. M.; Blaauw, R.; Meetsma, A.; Teuben, J. H.; Gyepes, R.; Varga, V.; Mach, K.; Veldman, N.; Spek, A. *Organometallics* **1996**, *15*, 4977.
(36) Sanner, R. D.; Duggan, M. D.; McKenzie, T. C.; Marsh, R. E.; Bercaw, J. E. *J. Am. Chem. Soc.* **1976**, *98*, 8358.
(37) Duchateau, R.; Gambarotta, S.; Beydoun, N.; Bensimon, C. *J. Am. Chem. Soc.* **1991**, *113*, 8986.
(38) Beydoun, N.; Duchateau, R.; Gambarotta, S. *J. Chem. Soc., Chem. Commun.* **1992**, 244.
(39) Dunn, S. C.; Batsanov, A. S.; Mountford, P. *J. Chem. Soc., Chem. Commun.* **1994**, 2007.

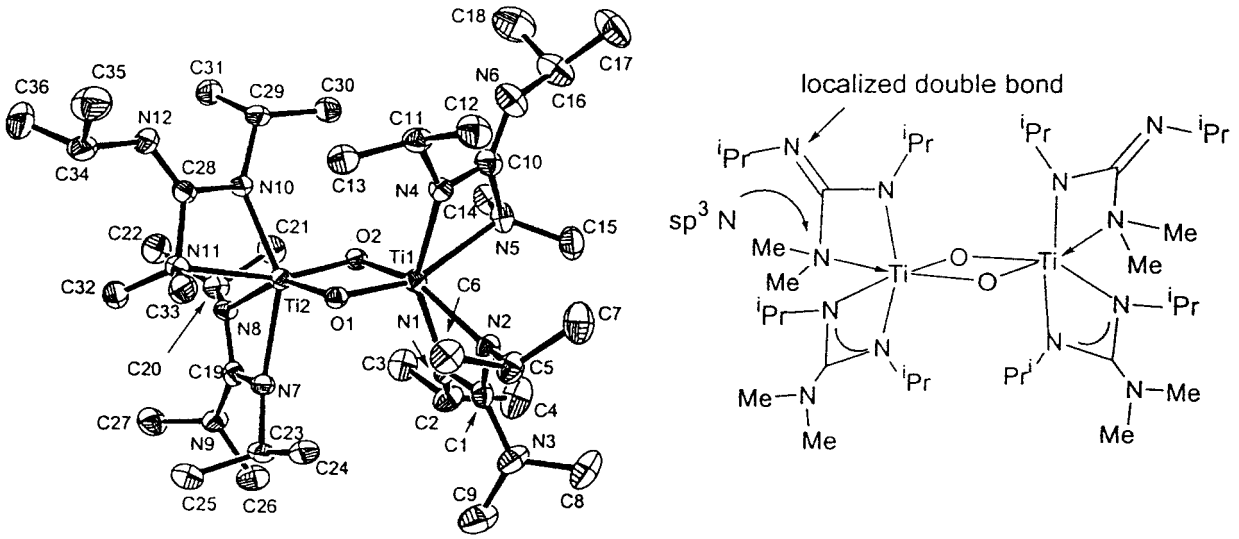

Figure 10. ORTEP diagram of **4**, showing 50% thermal probability ellipsoids. Hydrogen atoms are omitted for clarity. Line drawing depicting bonding in **4**.

Table 5. Selected Bond Lengths (Å) and Angles (deg) for **4**

Ti(1)	O(1)	1.760(2)		Ti(1)	O(2)	1.915(2)	
Ti(1)	N(1)	2.152(3)		Ti(1)	N(2)	2.123(3)	
Ti(1)	N(4)	2.012(3)		Ti(1)	N(5)	2.355(3)	
Ti(2)	O(1)	1.933(2)		Ti(2)	O(2)	1.769(2)	
Ti(2)	N(7)	2.152(3)		Ti(2)	N(8)	2.112(3)	
Ti(2)	N(10)	2.014(3)		Ti(2)	N(11)	2.343(3)	
N(1)	C(1)	1.328(5)		N(7)	C(19)	1.322(5)	
N(2)	C(1)	1.339(5)		N(8)	C(19)	1.338(5)	
N(3)	C(1)	1.399(5)		N(9)	C(19)	1.393(5)	
N(4)	C(10)	1.371(5)		N(10)	C(28)	1.363(5)	
N(5)	C(10)	1.484(4)		N(11)	C(28)	1.481(5)	
N(6)	C(10)	1.275(4)		N(12)	C(28)	1.288(5)	
O(1)	Ti(1)	O(2)	83.5(1)	O(1)	Ti(1)	N(1)	109.2(1)
O(1)	Ti(1)	N(2)	102.0(1)	O(1)	Ti(1)	N(4)	100.3(1)
O(1)	Ti(1)	N(5)	160.0(1)	O(1)	Ti(1)	C(1)	106.1(1)
O(2)	Ti(1)	N(1)	89.5(1)	O(2)	Ti(1)	N(2)	151.6(1)
O(2)	Ti(1)	N(4)	106.8(1)	O(2)	Ti(1)	N(5)	92.7(1)
O(2)	Ti(1)	C(1)	120.3(1)	N(1)	Ti(1)	N(2)	62.3(1)
N(1)	Ti(1)	N(4)	147.9(1)	N(1)	Ti(1)	N(5)	90.4(1)
N(2)	Ti(1)	N(4)	99.7(1)	N(2)	Ti(1)	N(5)	90.8(1)
N(4)	Ti(1)	N(5)	61.9(1)	O(1)	Ti(2)	O(2)	82.7(1)
O(1)	Ti(2)	N(7)	89.7(1)	O(1)	Ti(2)	N(8)	151.8(1)
O(1)	Ti(2)	N(10)	106.3(1)	O(1)	Ti(2)	N(11)	91.4(1)
O(2)	Ti(2)	N(7)	108.7(1)	O(2)	Ti(2)	N(8)	103.5(1)
O(2)	Ti(2)	N(10)	98.7(1)	O(2)	Ti(2)	N(11)	157.6(1)
N(7)	Ti(2)	N(8)	62.2(1)	N(7)	Ti(2)	N(10)	149.9(1)
N(7)	Ti(2)	N(11)	92.8(1)	N(8)	Ti(2)	N(10)	100.0(1)
N(8)	Ti(2)	N(11)	91.9(1)	N(10)	Ti(2)	N(11)	62.2(1)
Ti(1)	O(1)	Ti(2)	96.7(1)	Ti(1)	O(2)	Ti(2)	97.0(1)
N(1)	C(1)	N(3)	126.0(4)	N(4)	C(10)	N(5)	105.0(3)
N(4)	C(10)	N(6)	125.6(3)	N(5)	C(10)	N(6)	129.3(4)
N(7)	C(19)	N(8)	111.7(3)	N(10)	C(28)	N(11)	105.7(3)
N(10)	C(28)	N(12)	123.3(4)	N(11)	C(28)	N(12)	131.0(4)

the rearranged guanidinate ligands show a localized bonding situation (Figure 10). The bonds between the central carbons and the noncoordinated nitrogens of the asymmetrically bound guanidinates (C10−N6, 1.275(5) Å and C28−N12, 1.288(5) Å) are similar to the sp^2C-sp^2N double bonds, such as those observed in imines ($C{=}N_{av}$, 1.28 Å).[40] The amide nitrogen atoms bound to titanium are planar, and the C−N distances (C10−N4, 1.371(5) Å and C28−N10, 1.363(5) Å) are consistent with known sp^2C-sp^2N single bonds ($C-N_{av}$, 1.355 Å).[41] Finally, the dimethylamino nitrogen atoms bonded to titanium have tetrahedral geometries, and the bonds to the central carbon (C10−N5, 1.484(5) Å and C28−N11, 1.480(5) Å) are longer than expected for sp^2C-sp^3N single bonds ($C-N_{av}$, 1.416).[41] These bonds are closer to distances reported for sp^3C-sp^3N single bonds ($C-N_{av}$, 1.469),[41] which may be due to the geometrical constraints of the metallacycle.

The room temperature ^1H NMR spectrum of **4** in C_6D_6 indicates that the new guanidinate coordination mode observed in the solid state is retained in solution. An additional C_2 symmetry axis perpendicular to the Ti_2O_2 core is also present. This symmetry results in the appearance of only eight isopropyl methyl group resonances and three *N*-methyl group (6H:6H:12H) resonances. The two resonances integrating to 6H correspond to the diastereotopic methyl groups on the amino nitrogen atoms bound to titanium, whereas the resonance which integrates to 12H corresponds to the *N*-methyl protons on the symmetrically bound guanidinate ligands. When a sample of **4** in toluene-d_8 is cooled, the ^1H NMR spectrum sharpens, but otherwise the resonances do not change. Upon heating, the ligand resonances broaden and begin to coalesce; however, the process is still incomplete up to 89 °C. These data suggest that it is possible for the guanidinates to interconvert between the symmetrical and asymmetrical coordination modes at high temperature. Although this process is reversible upon returning the sample to room temperature, significant thermal decomposition of **4** is also observed during the experiment.

Complex **4** does not react with bases such as pyridine or DMAP. Additionally, neither **4** nor the dinitrogen complex **2** reacts with excess pyridine *N*-oxide, to afford a base-trapped terminal oxo complex, as is precedented in related amidinate-supported titanium complexes.[7] These experiments indicate that a monomeric titanium oxo complex is not readily accessible from **2** or **4**.

The sulfur analogue of **4**, $\{[Me_2NC(N^iPr)_2]_2TiS\}_2$ (**5**), was synthesized by treating the dinitrogen complex **2** with 2 equiv of propylene sulfide (eq 5).

$$2 \xrightarrow[\text{Toluene}]{2\ \overset{S}{\triangle}} \underset{\mathbf{5}}{\{[Me_2NC(N^iPr)_2]_2TiS\}_2} \qquad (5)$$

The solid-state structure of **5** (Figure 11) shows bonding features similar to those observed in complex **4**. One symmetrically and

(40) March, J. In *Advanced Organic Chemistry*; McGraw-Hill: New York, 1977; Vol. 2, p 24.

(41) *Handbook of Chemistry and Physics*; 77 ed.; Lide, D. R., Ed. CRC Press: Boca Raton, 1996.

Table 6. Crystallographic Data and Refinement Details for **4**−**6**[a]

	4	**5**	**6**
empirical formula	$C_{36}H_{80}N_{12}Ti_2O_2$	$C_{36}H_{80}N_{12}Ti_2S_2$	$C_{18}H_{40}N_6TiS_2$
formula weight	808.91	841.03	452.57
temp (°C)	−118	−110	−115
cryst syst	triclinic	monoclinic	monoclinic
space group	$P\bar{1}$ (#2)	$P2_1/c$ (#14)	$P2_1/n$ (#14)
a (Å)	9.2058(5)	12.5628(7)	9.0710(8)
b (Å)	11.3193(6)	21.703(1)	16.006(1)
c (Å)	23.773(1)	17.5569(9)	16.918(1)
V (Å^3)	2426.8(2)	4766.1(4)	2453.9(3)
α (deg)	83.430(1)	90	90
β (deg)	80.486(1)	95.347(1)	92.565(1)
γ (deg)	87.943(1)	90	90
Z	2	4	4
d_{calc} (g/cm^3)	1.107	1.172	1.225
diffractometer	Siemens SMART	Siemens SMART	Siemens SMART
radiation	Mo Kα	Mo Kα	Mo Kα
monochromator	graphite	graphite	graphite
detector	CCD area	CCD area	CCD are
scan type, deg	ω, 0.3	ω, 0.3	ω, 0.3
frame collection time (s)	10	10	10
reflections measured	hemisphere	hemisphere	hemisphere
2θ range (deg)	3−52.3	3−52.1	3−52.4
μ (mm^{-1})	3.70	4.60	5.34
T_{max}, T_{min}	0.914, 0.735	0.931, 0.787	0.931, 0.510
crystal dimensions (mm)	0.21 × 0.22 × 0.11	0.14 × 0.28 × 0.48	0.29 × 0.18 × 0.11
no. reflns measured	13410	22075	11864
no. unique reflns	8242	8710	4538
no. observations (I>3σ)	4501	3810	2213
no. variables	496	469	400
data/parameter	9.07	8.12	5.53
refinement method	full-matrix least-squares on F^2	full-matrix least-squares on F^2	full-matrix least-squares on F^2
*R*int (%)	3.3	5.0	6.9
R (%)	4.4	4.2	3.4
*R*w (%)	4.7	4.4	3.5
GOF	1.34	1.36	1.07
largest diff. peak and hole e Å^{-3}	0.48 −0.36	0.76 −0.34	0.42 −0.21
hydrogen atoms	ideal. positions	ideal. positions	ideal. positions

[a] $R = [\Sigma||F_o| - |F_c||]/\Sigma|F_o|$, $Rw = \{[\Sigma w(|F_o| - |F_c|)^2]/\Sigma w|F_o^2|\}^{1/2}$, $GOF = \{[\Sigma w(|F_o| - |F_c|)^2]/(n_o - n_v)\}^{1/2}$.

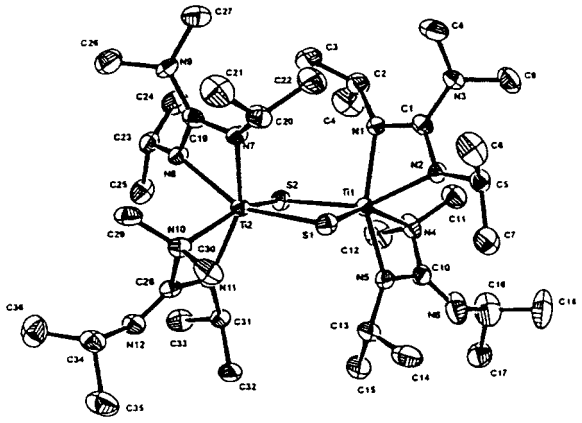

Figure 11. ORTEP diagram of **5**, showing 50% thermal probability ellipsoids. Hydrogen atoms are omitted for clarity.

one asymmetrically bound guanidinate are present on each titanium center. The Ti_2S_2 core is bent slightly (twist angle S1−Ti1−S2/S1−Ti2−S2, 171°) and has pairs of short and long Ti−S distances; as in **4**, the short Ti−S bonds are trans to the dimethylamino nitrogen atoms. Important bond angles and distances are listed in Table 7; selected crystal and refinement details are given in Table 6.

The solution behavior of **5** is much more complex than that of the oxo derivative **4**, as it is both solvent and temperature dependent. The variable-temperature ^{1}H NMR spectra indicate that multiple exchange processes may interconvert the several different species present. At room temperature in benzene-d_6 or toluene-d_8, the ^{1}H NMR spectrum exhibits broad resonances for the isopropyl methyl groups and both one sharp and one broad resonance for the methine protons and the *N*-methyl resonances. When a sample of **5** in toluene-d_8 was cooled to −80 °C, many sharp peaks were observed in the ^{1}H NMR spectrum, possibly due to the formation of aggregates or restricted intramolecular fluxional processes. Heating the sample to 74 °C caused partial coalescence of some of the peaks; however, some resonances remained unchanged, and the thermal decomposition of **5** was also observed. Upon returning the sample to room temperature, free diisopropyl carbodiimide and a singlet (δ 3.7 ppm) consistent with a Ti−NMe_2 group were observed among the degradation products. ^{1}H NMR spectra in THF-d_8, pyridine-d_5, or acetonitrile-d_3 do not show evidence for a cleanly trapped species; rather, a complex mixture of resonances is observed in each case.

In contrast to the behavior described above, the ^{1}H NMR spectra of **5** in chlorinated solvents (CD_2Cl_2, $CDCl_3$, $CDCl_2F$) exhibit resonances consistent with a single species with symmetrically bound guanidinate ligands. This is further supported by the variable temperature NMR spectra in CD_2Cl_2. At high temperature (55 °C), coalescence to a single resonance is observed for the isopropyl methyl groups, while at the decoalesence temperature (−65 °C), four doublets are observed. A sample of **5** in $CDCl_2F$[42] at −126 °C did not reveal any further

Scheme 1

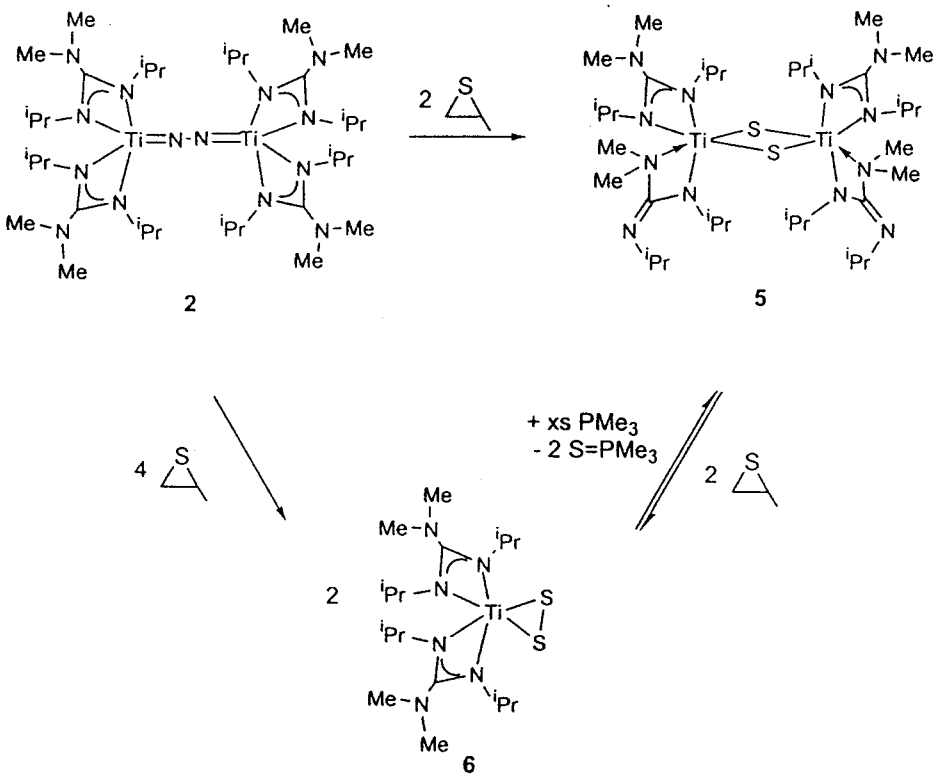

Table 7. Selected Bond Lengths (Å) and Angles (deg) for **5**

Ti(1)	S(1)	2.268(2)	Ti(1)	S(2)	2.397(2)
Ti(1)	N(1)	2.145(4)	Ti(1)	N(2)	2.108(4)
Ti(1)	N(4)	2.375(4)	Ti(1)	N(5)	1.986(4)
Ti(2)	S(1)	2.406(2)	Ti(2)	S(2)	2.270(2)
Ti(2)	N(7)	2.125(4)	Ti(2)	N(8)	2.092(4)
Ti(2)	N(10)	2.388(4)	Ti(2)	N(11)	1.993(4)
N(1)	C(1)	1.329(6)	N(7)	C(19)	1.329(6)
N(2)	C(1)	1.332(5)	N(8)	C(19)	1.357(5)
N(3)	C(1)	1.394(6)	N(9)	C(19)	1.381(6)
N(4)	C(10)	1.486(7)	N(10)	C(28)	1.476(6)
N(5)	C(10)	1.356(6)	N(11)	C(28)	1.378(5)
N(6)	C(10)	1.292(7)	N(12)	C(28)	1.267(5)

S(1)	Ti(1)	S(2)	90.28(6)	S(1)	Ti(1)	N(1)	114.0(1)
S(1)	Ti(1)	N(2)	100.0(1)	S(1)	Ti(1)	N(4)	155.2(1)
S(1)	Ti(1)	N(5)	94.7(1)	S(2)	Ti(1)	N(1)	88.6(1)
S(2)	Ti(1)	N(2)	150.9(1)	S(2)	Ti(1)	N(4)	98.9(1)
S(2)	Ti(1)	N(5)	103.7(1)	N(1)	Ti(1)	N(2)	62.4(1)
N(1)	Ti(1)	N(4)	89.4(1)	N(1)	Ti(1)	N(5)	148.9(2)
N(2)	Ti(1)	N(4)	83.0(1)	N(2)	Ti(1)	N(5)	102.4(2)
N(4)	Ti(1)	N(5)	60.8(2)	S(1)	Ti(2)	S(2)	89.99(6)
S(1)	Ti(2)	N(7)	85.5(1)	S(1)	Ti(2)	N(8)	147.9(1)
S(1)	Ti(2)	N(10)	99.36(10)	S(1)	Ti(2)	N(11)	105.4(1)
S(2)	Ti(2)	N(7)	115.5(1)	S(2)	Ti(2)	N(8)	98.4(1)
S(2)	Ti(2)	N(10)	157.0(1)	S(2)	Ti(2)	N(11)	96.3(1)
N(7)	Ti(2)	N(8)	62.9(1)	N(7)	Ti(2)	N(10)	86.3(1)
N(7)	Ti(2)	N(11)	146.6(2)	N(8)	Ti(2)	N(10)	84.8(1)
N(8)	Ti(2)	N(11)	104.3(1)	N(10)	Ti(2)	N(11)	61.0(1)
Ti(1)	S(1)	Ti(2)	89.47(5)	Ti(1)	S(2)	Ti(2)	89.68(5)
N(1)	C(1)	N(2)	111.7(4)	N(4)	C(10)	N(5)	103.5(4)
N(4)	C(10)	N(6)	131.9(6)	N(5)	C(10)	N(6)	124.6(6)
N(7)	C(19)	N(8)	109.9(4)	N(10)	C(28)	N(11)	104.0(4)
N(10)	C(28)	N(12)	129.9(4)	N(11)	C(28)	N(12)	126.1(4)

changes from the −65 °C spectrum. The data from ^{1}H−^{1}H TOCSY and ^{1}H−^{1}H NOESY experiments in CD_2Cl_2 at −65 °C were analogous to those for complexes **1** and **2**. These data are consistent with symmetrically bound ligands at all temperatures, which are subject to the processes of fast racemization and ligand rotation discussed previously for complexes **1**, **2**, and **3**. Due to the high solubility of **5** in the halogenated solvents, attempts to crystallize the species observed in these solvents were unsuccessful.

Cycles of dissolution and evaporation of solvent from **5**, alternating between C_6D_6 and CD_2Cl_2 solvents, show complete reversibility in the ^{1}H NMR spectral features. Additionally, upon titration of a room-temperature C_6D_6 solution of **5** with CD_2Cl_2, the ^{1}H NMR resonances change to a spectrum similar to that of **5** in pure CD_2Cl_2. Approximately 60 equiv (100 μL) of methylene chloride are required to observe significant changes in the spectrum.

The nature of the solvent-induced behavior observed for the sulfido complex **5** is puzzling. For nonhalogenated solvents (C_6D_6, toluene-d_8, THF-d_8, pyridine-d_5, acetonitrile-d_3), no spectral trends can be discerned that are controlled by the dielectric constant or the donor properties of the solvent. There may be multiple equilibrating products and/or intramolecular fluxional processes occurring in these solvents. The halogenated solvents (CD_2Cl_2, $CDCl_3$, $CDCl_2F$) are in the middle of the range of dielectric constants and are typically very poor donors to metals, yet in these solvents, **5** appears to be a single species with symmetrical ligands. This may be either a monomeric terminal sulfido complex or a dimer with two bridging sulfido ligands. Solution molecular weight determination experiments[43] were inconclusive due to decomposition of **5** over several days in solution.

Given the possibility of multiple equilibria in solution, we further probed the behavior of complex **5** by its reactivity with organic substrates. The addition of 2 equiv of propylene sulfide

(42) The ^{1}H NMR spectra of **6** in $CDCl_2F$ from −65 to 25 °C are similar to those in CD_2Cl_2.

(43) The Signer method for solution molecular weight determination was used. See: Burger, B. J., Bercaw, J. E. In *Experimental Organometallic Chemistry*; Wayda, A. L., Ed.; American Chemical Society: Washington D.C., 1987; p 94.

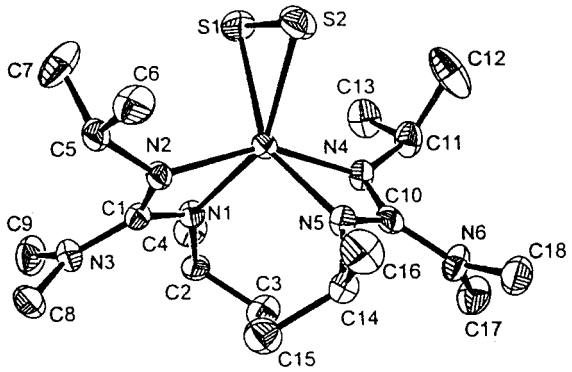

Figure 12. ORTEP diagram of **6**, showing 50% thermal probability ellipsoids. Hydrogen atoms are omitted for clarity.

Table 8. Selected Bond Lengths (Å) and Angles (deg) for **6**

Ti(1)	S(1)		2.330(1)	Ti(1)	S(2)		2.332(1)
Ti(1)	N(1)		2.097(3)	Ti(1)	N(2)		2.080(3)
Ti(1)	N(4)		2.075(3)	Ti(1)	N(5)		2.085(3)
S(1)	S(2)		2.091(2)				
S(1)	Ti(1)	S(2)	53.31(4)	S(1)	Ti(1)	N(1)	103.13(8)
S(1)	Ti(1)	N(2)	102.45(9)	S(1)	Ti(1)	N(4)	102.84(9)
S(1)	Ti(1)	N(5)	148.23(9)	S(2)	Ti(1)	N(1)	151.61(9)
S(2)	Ti(1)	N(2)	102.61(9)	S(2)	Ti(1)	N(4)	102.97(9)
S(2)	Ti(1)	N(5)	99.38(8)	N(1)	Ti(1)	N(2)	63.9(1)
N(1)	Ti(1)	N(4)	97.5(1)	N(1)	Ti(1)	N(5)	107.2(1)
N(2)	Ti(1)	N(4)	151.5(1)	N(2)	Ti(1)	N(5)	99.1(1)
N(4)	Ti(1)	N(5)	64.3(1)	Ti(1)	S(1)	S(2)	63.40(4)
Ti(1)	S(2)	S(1)	63.29(4)				

to **5** yields the monomeric η^2-persulfido complex **6**.[44] ^{1}H NMR and X-ray crystallographic studies (see below) indicate the guanidinate ligands are symmetrically bound both in solution and solid state (Figure 12). Addition of 2 or more equiv of PMe_3 to **6** results in regeneration of **5** along with 2 equiv of $S{=}PMe_3$ (Scheme 1). Notably, even in the presence of excess phosphine, only the dimer **5** is obtained; no evidence for a terminal sulfido complex with coordinated PMe_3 is observed.

Other substrates can be used to cleave the sulfido dimer **5**, including carbodiimides, 4-(dimethylamino)pyridine, and pyridine *N*-oxide (Scheme 2). The reactions with carbodiimides yield azathiatitanacyclobutanes (**7**, **8**), whereas the latter two reagents produce monomeric terminal sulfido complexes with coordinated base (**9**, **10**). The guanidinate ligands in all of the resulting complexes are symmetrically bound to the titanium atom.

X-ray Studies of Monomeric Complexes with Symmetrically Bound Guanidinate Ligands. Inspection of the X-ray crystal structures of the dichloride **1**, dinitrogen compound **2**, imido **3**, and persulfido **6** shows several noteworthy features. Important bond angles and distances for **6** are listed in Table 8 (key metrical parameters for the guanidinate ligands **1**−**3** and **6** are summarized in Table 9). The twist angles between the N−Ti−N and N−C−N planes indicate that the metallacycles are nearly planar and that each guanidinate ligand is chelated to titanium in a σ fashion. There is no significant contribution from the delocalized π system. In all cases, the central carbon and the uncoordinated nitrogen of the guanidinate are planar (sum of angles 359.8−360°). Inspection of the angles around the nitrogen atoms coordinated to titanium reveals that while most atoms are very close to planar, others deviate significantly (sum of angles 343.4−360°). This range of geometries may be due to steric or packing effects in the solid state.

Scheme 2

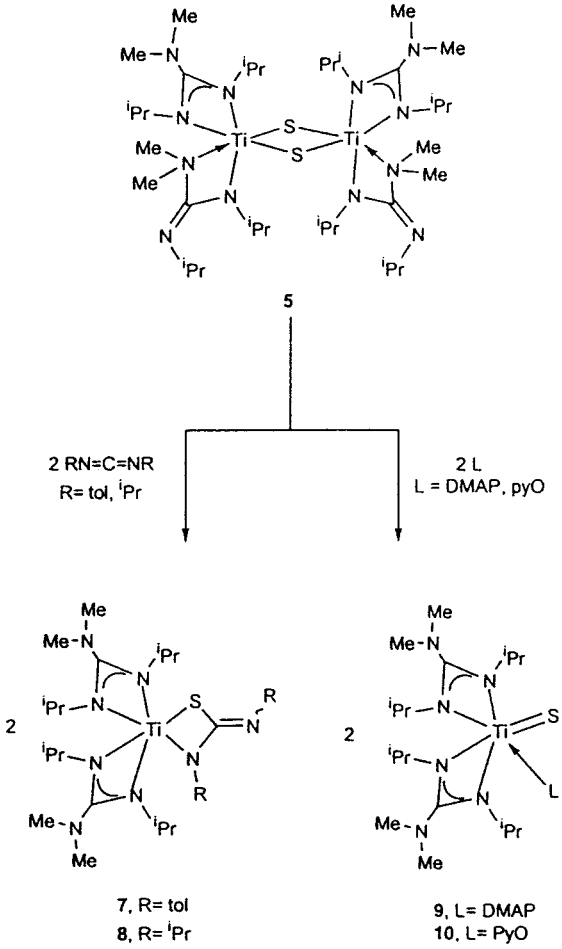

Charge delocalization within the chelated portion of the guanidinate is evident from the C−N bond lengths, which range from 1.31(1) to 1.358(8) Å; within a given guanidinate, these two bonds are statistically equivalent. These data are similar to C−N bond distances reported for related metal amidinate complexes.[45,46] Although the dihedral angles (28−48°) suggest that the methyl groups on the noncoordinated nitrogen atom hinder optimal alignment of the nitrogen lone pair with the π system of the chelate atoms, the bond distances between the central carbon (C1 or C10) to the noncoordinated nitrogen (N3 or N6), which range from 1.371(4) to 1.40(1) Å, suggest that charge delocalization extends throughout the N_3C guanidinate core. While these bonds are elongated relative to the chelate C−N bonds, they are still shorter than typical C−N single bonds.

Summary

The *N*,*N*′-diisopropyl-*N*″,*N*″-dimethylguanidinate ligand has been used to support a reduced titanium center, leading to the synthesis of the bridging dinitrogen complex **2**. The latter undergoes heteroatom abstraction reactions with nitrogen-, oxygen-, and sulfur-containing substrates to yield imido (**3**), bridging dioxo (**4**), and bridging disulfido (**5**) complexes. The guanidinate ligands in **4** and **5** rearrange to form complexes with a novel asymmetrical coordination mode. This rearrangement is reversible for complex **5**; the rearrangement and

(44) Complex **7** can be independently synthesized by addition of 4 equiv elemental sulfur to dinitrogen complex **3**.

(45) Barker, J.; Kilner, M. *Coord. Chem. Rev.* **1994**, *133*, 219.
(46) Edelmann, F. T. *Coord. Chem. Rev.* **1994**, *133*, 137.

Table 9. Summary of Metrical Parameters for Symmetrically Bound Guanidinate Ligands

	guan$_2$TiCl$_2$ **1**	[guan$_2$Ti]$_2$(N$_2$) **2**	guan$_2$TiNPh **3**	guan$_2$TiS$_2$ **6**
		Bond Lengths (Å)		
C1−N1	1.329(8)	1.33(1)	1.342(3)	1.337(4)
C1−N2	1.349(8)	1.34(1)	1.348(3)	1.341(4)
C10−N4	1.339(8)	1.31(1)	n/a	1.337(4)
C10−N5	1.358(8)	1.34(1)	n/a	1.347(5)
C1−N3	1.393(8)	1.39(1)	1.372(3)	1.371(4)
C10−N6	1.380(8)	1.40(1)	n/a	1.378(5)
		Dihedral Angle (°)		
N2−C1−N3−C8	37.0(3)	−28(1)	−31.7(3)	−38.4
N4−C10−N6−C17	39.4(3)	−48(1)	n/a	−35.9(6)
		Twist Angle (°)		
N1−Ti1−N2/N1−C1−N2	178.77	174.36	179.93	179.74
N4−Ti1−N5/N4−C10−N5	176.76	174.91	n/a	178.81

intramolecular fluxionality and isomerization of the complexes was studied with symmetrically bound ligands.

Experimental Section

General Considerations. Standard Schlenk line and glovebox techniques were used throughout. Tetrahydrofuran and diethyl ether were distilled from purple Na/benzophenone under nitrogen. Pyridine was distilled from Na under nitrogen. Benzene, hexane, and pentane were dried by passage through activated alumina.[47] C_6D_6, toluene-d_8, and THF-d_8 were vacuum transferred from Na/benzophenone. Pyridine-d_5 was vacuum transferred from sodium. Acetonitrile-d_3, methylene chloride-d_2, and chloroform-d_1 were vacuum transferred from CaH_2. $CDCl_2F$ was prepared according to the literature procedure,[48] dried over CaH_2, and stored over molecular sieves in a thick-walled Teflon-sealed flask at 5 °C. Propylene sulfide (Aldrich) and cyclohexene sulfide (Aldrich) were first dried over molecular sieves, then transferred under static vacuum to a Teflon sealed flask, and stored at 5 °C. Diisopropylcarbodiimide (Lancaster) was distilled from CaH_2. Pyridine *N*-oxide (Aldrich) was dried over molecular sieves in toluene, and the crude solid was sublimed before use. Di(*p*-tolyl)carbodiimide (Aldrich), dicyclohexylcarbodiimide (Aldrich), $LiNMe_2$ (Strem), Mg powder (Strem), xylylisocyanide (Fluka), and 4-(dimethylamino)pyridine (Lancaster) were used as received. $TiCl_2(NMe_2)_2$ was prepared according to the literature procedure.[49] IR samples were prepared as mineral oil mulls and taken between KBr plates. Elemental analysis and mass spectral data were determined by the College of Chemistry, University of California, Berkeley, CA. Single-crystal X-ray determinations were performed at CHEXRAY, University of California, Berkeley, CA. Repeated attempts to obtain satisfactory $^{13}C\{^1H\}$ NMR spectra for the fluxional compounds **2**, **4**, **5**, and **8** were unsuccessful.

[Me$_2$NC(N^{i}Pr)$_2$]$_2$TiCl$_2$ (1). A 100 mL round-bottomed flask was charged with $(Me_2N)_2TiCl_2$ (0.700 g, 3.38 mmol). Et_2O (45 mL) was added by cannula, and the red−orange solution was cooled to −20 °C. Diisopropylcarbodiimide (1.2 mL, 7.7 mmol) was added by syringe, and the reaction mixture was allowed to warm to room-temperature overnight. The red solution was concentrated to dryness, producing **1** as a spectroscopically pure (^{1}H NMR) microcrystalline solid **1** in >95% yield. Recrystallization of **1** from Et_2O at −30 °C overnight yielded red crystals that were isolated by filtration (0.830 g, two crops, 53%). ^{1}H NMR (C_6D_6, 500 MHz): δ 1.60 (br, 24H, NCH(CH_3)$_2$), 2.31 (s, 12 H, N(CH_3)$_2$), 3.70 (br, 4H, NCH(CH$_3$)$_2$). $^{13}C\{^1H\}$NMR (C_6D_6, 125 MHz): δ 24.4 (br, NCH(*C*H$_3$)$_2$, 40.0 (s, N*C*H$_3$), 50.6 (s, N*C*H(CH$_3$)$_2$), 172.0 (s, N$_3$*C*). IR (cm^{-1}): 2962 (s), 2925 (s), 2857 (s), 1530 (m), 1462 (s), 1423 (m), 1395 (m), 1347 (m), 1312 (w), 1280 (w), 1184 (m), 1127 (w), 1058 (m), 933(w), 740 (w), 724 (w), 705 (w), 540 (w). Anal. Calcd for $C_{18}H_{40}N_6Cl_2Ti$: C, 47.08; H, 8.78; N, 18.30. Found: C, 47.39; H, 8.94; N, 18.09.

{**[Me$_2$NC(N^{i}Pr)$_2$]$_2$Ti**}$_2$**(N$_2$) (2).** A 500 mL round-bottomed flask was charged with [Me$_2$NC(N^{i}Pr)$_2$]$_2$TiCl$_2$ (12.0 g, 2.61 mmol) and Mg powder (6.35 g, 26.1 mmol). The solids were cooled to −40 °C, and THF (450 mL) was added. The red solution was allowed to slowly warm to room temperature with stirring under a flow of dinitrogen overnight. The resulting purple solution was filtered from the excess Mg powder, and the volatile materials were removed under reduced pressure. The solid was extracted into pentane (1 × 350 mL, 1 × 100 mL), and the resulting purple solution was filtered through a fritted disk with a pad of Celite. The filtrate was concentrated to approximately 100 mL and cooled to −30 °C. Dark purple crystals were isolated by filtration (5.66 g, two crops, 54%). ^{1}H NMR (C_6D_6, 500 MHz): δ 1.42 (br, 48 H, NCH(CH_3)$_2$), 2.66 (s, 24 H, N(CH_3)$_2$), 3.85 (br, 8H, NCH(CH$_3$)$_2$). IR (cm^{-1}): 2955 (s), 2930 (s), 2857 (s), 1512 (m), 1403 (m), 1403 (m), 1334 (w), 1318 (w), 1185 (s), 1171 (w), 1139(w), 1122 (w), 1052 (m), 942 (w), 866 (w), 738 (w), 722 (w), 547 (w). Anal. Calcd for $C_{36}H_{80}N_{14}Ti_2$: C, 53.75; H, 10.02; N, 24.39. Found: C, 54.13; H, 10.42; N, 24.47.

[Me$_2$NC(N^{i}Pr)$_2$]$_2$TiNPh (3). {[Me$_2$NC(N^{i}Pr)$_2$]$_2$Ti}$_2$(N$_2$) (0.154 g, 0.191 mmol) was weighed into a 100 mL round-bottomed flask and dissolved in 20 mL of toluene. The solution was cooled to −65 °C, and a solution of 1.93 equiv PhN_3 (0.044 g, 0.37 mmol) in toluene (25 mL) was added slowly by cannula transfer. The solution immediately turned red and rapid bubbling was observed. After 1 h, the volatile materials were removed under reduced pressure to afford a spectroscopically pure (^{1}H NMR) orange red solid, [Me$_2$NC(N^{i}Pr)$_2$]$_2$TiNPh. The solid was recystallized from Et_2O at −30 °C to afford orange red crystals (0.095 g, 50%). ^{1}H NMR (C_6D_6, 500 MHz): δ 1.38 (d, J = 6 Hz, 24 H, NCH(CH_3)$_2$), 2.44 (s, 12 H, N*C*H$_3$), 3.64 (sept, J = 6 Hz, 4H, NCH(CH$_3$)$_2$), 6.67 (m, 1H, Ar), 7.09 (br, 2H, Ar), 7.10 (d, J = 8 Hz, 2H, Ar). $^{13}C\{^1H\}$NMR (C_6D_6, 125 MHz): δ 25.7 (s, NCH(*C*H$_3$)$_2$), 39.5 (s, N(*C*H$_3$)$_2$), 48.9 (s, N*C*H(CH$_3$)$_2$), 119.4 (Ar), 125.8 (Ar), 161.8 (Ar), 169.2 (N$_3$*C*). IR (cm^{-1}): 2954 (s), 2919 (s), 2853 (s), 1640 (m), 1578 (m), 1519 (m), 1462 (m), 1398 (m), 1337 (m) 1317 (m), 1171 (m), 1123 (m), 1053 (m), 1010 (w), 963 (w), 750 (m). Anal. Calcd for $C_{24}H_{45}N_7Ti$: C, 60.10; H, 9.46; N, 20.46. Found: C, 60.40; H, 9.37; N, 20.26.

{**[Me$_2$NC(N^{i}Pr)$_2$]$_2$TiO**}$_2$ **(4).** A 100 mL round-bottomed flask was charged with {[Me$_2$NC(N^{i}Pr)$_2$]$_2$Ti}$_2$(N$_2$) (0.300 g, 0.373 mmol). The solid was dissolved in toluene (30 mL), and the solution was cooled to −65 °C. A solution of pyridine *N*-oxide (0.071 g, 0.736 mmol) in toluene (15 mL) was added dropwise. After the addition was complete, the solution was slowly warmed to room-temperature overnight. The resulting yellow−brown solution was concentrated to a solid residue, and the product was extracted into Et_2O (50 mL). The solution was filtered through a fritted disk with a Celite pad. The filtrate was concentrated and cooled to −35 °C. Bright yellow crystals were isolated by filtration (0.214 g, two crops, 71%). ^{1}H NMR (273K, C_7D_8, 500 MHz): δ 1.10 (d, J = 6 Hz, 6H, NCH(CH_3)$_2$), 1.29 (d, J = 6 Hz, 12 H, NCH(CH_3)$_2$), 1.32 (d, J = 6 Hz, 6H, NCH(CH_3)$_2$), 1.53 (d, J = 6 Hz, 6H, NCH(CH_3)$_2$), 1.61 (d, J = 6 Hz, 6H, NCH(CH_3)$_2$), 1.67 (d, J = 6 Hz, 6H, NCH(CH_3)$_2$), 1.81 (d, J = 6 Hz, 6H, NCH(CH_3)$_2$), 2.50 (br, 12H, N*C*H$_3$), 2.60 (s, 6H, N(CH$_3$)(CH_3)), 2.73 (s, 6H, N(CH_3)-(CH$_3$)), 3.61 (sept, J = 6 Hz, 2H, NCH(CH$_3$)$_2$), 3.73 (sept, J = 6 Hz, 2H, NCH(CH$_3$)$_2$), 3.99 (sept, J = 6 Hz, 2H, NCH(CH$_3$)$_2$), 4.30 (sept, J = 6 Hz, 2H, NCH(CH$_3$)$_2$). IR (cm^{-1}): 1622 (s), 1514 (s), 1462 (s), 1405 (m), 1339 (w), 1314 (w), 1273 (s), 1196 (m), 1171 (m), 1123 (m), 1055 (m), 1005 (m), 916 (w), 885 (w), 758 (s), 738 (s), 548 (m),

(47) Alaimo, P. J.; Peters, D. W.; Arnold, J.; Bergman, R. G. *J. Chem. Educ.* **2001**, *78*, 64.
(48) Siegel, J. S.; Anet, F. A. L. *J. Org. Chem.* **1988**, *53*, 2629.
(49) Benzing, E.; Kornicker, W. *Chem. Ber.* **1961**, *94*, 3.

476 (w), 432 (m). EI−MS (*m*/*z*): 639 (M − guanidinate), 512 (M − guanidinate, ^{i}PrNCN^{i}Pr), 468 (M − 2guanidinate). Anal. Calcd for $C_{36}H_{80}N_{12}O_2Ti_2$: C, 53.44; H, 9.97; N, 20.79. Due to the presence of solvent, repeated attempts to obtain satisfactory analysis were unsuccessful.

{[Me$_2$NC(N^{i}Pr)$_2$]$_2$TiS}$_2$ (5). A 250 mL round-bottomed flask was charged with {[Me$_2$NC(N^{i}Pr)$_2$]$_2$Ti}$_2$(N$_2$) (1.77 g, 2.20 mmol). Toluene (140 mL) was added, and the solution was cooled to −10 °C. Propylene sulfide (0.340 mL, 4.33 mmol) was added by syringe, and the solution was warmed to room temperature. After 4 h, the volatile materials were removed under reduced pressure. The resulting solid was extracted with pentane (80 mL), filtered through a fritted disk with a pad of Celite, and concentrated to approximately 15 mL. Dark red crystals were isolated by filtration after cooling the solution to −30 °C (1.10 g, two crops, 60%). ^{1}H NMR (309 K, CD_2Cl_2, 500 MHz): δ 1.24 (b, 12H, NCH(C*H*$_3$)$_2$), 1.38 (b, 12H, NCH(C*H*$_3$)$_2$), 2.85 (s, 12H, N(C*H*$_3$)$_2$), 3.73 (sept, J = 6 Hz, 4H, NC*H*(CH$_3$)$_2$). IR (cm^{-1}): 1623 (s), 1525 (m), 1462 (s), 1404 (m), 1377 (m), 1334 (m), 1265 (m), 1190 (m), 1121 (w), 1055 (w), 1017 (m), 873 (w). Anal. Calcd for $C_{36}H_{80}N_{12}S_2Ti_2$: C, 51.41; H, 9.59; N, 19.99. Found: C, 51.54; H, 9.92; N, 19.91.

{[Me$_2$NC(N^{i}Pr)$_2$]$_2$TiS$_2$ (6). {[Me$_2$NC(N^{i}Pr)$_2$]$_2$Ti}$_2$(N$_2$) (0.350 g, 0.435 mmol) was dissolved in toluene (30 mL) in a 100 mL round-bottomed flask. Propylene sulfide (0.150 mL, 1.91 mmol) was added by microliter syringe. After 2 h, the deep green solution was concentrated to a solid. The residue was extracted with pentane (65 mL) and filtered to yield a green solution, which was concentrated to 15 mL. Dark green−blue crystals were isolated by filtration after cooling of the solution to −30 °C (0.160 g, 41%). ^{1}H NMR (C$_6$D$_6$, 500 MHz): δ 1.31 (d, J = 6 Hz, 24 H, NCH(C*H*$_3$)$_2$), 2.35 (s, 12 H, N(C*H*$_3$)$_2$), 3.60 (sept, J = 6 Hz, 4H, NC*H*(CH$_3$)$_2$). ^{13}C{^{1}H}NMR (C$_6$D$_6$, 125 MHz): δ 24.6 (br s, NCH(*C*H$_3$)$_2$), 39.9 (s, N*C*H$_3$), 48.6 (s, N*C*H-(CH$_3$)$_2$), 172.8 (N$_3$*C*). IR(cm^{-1}): 1518 (m), 1405 (m), 1338 (m), 1313 (w), 1185 (w), 1123 (w), 1052 (m), 745 (w), 725 (w). Anal. Calcd for $C_{18}H_{40}N_6S_2Ti$: C, 47.76; H, 8.91; N, 18.58. Found: C, 47.91; H, 9.13; N, 18.24.

{[Me$_2$NC(N^{i}Pr)$_2$]$_2$Ti[SC(NTol)$_2$] (7). Toluene (30 mL) was added to a mixture of {[Me$_2$NC(N^{i}Pr)$_2$]$_2$TiS}$_2$ (0.201 g, 0.239 mmol) and di-*p*-tolylcarbodiimide (0.108 g, 0.486 mmol). After stirring overnight, the solvent was removed under reduced pressure. The red oil was extracted with ether (70 mL) and filtered through a fritted disk with a pad of Celite. The solution was concentrated to 10 mL and cooled to −30 °C overnight. Deep red crystals were isolated by filtration (0.200 g, 65%). ^{1}H NMR (C$_6$D$_6$, 500 MHz): δ 0.97 (d, J = 6 Hz, 3H, NCH-(C*H*$_3$)$_2$), 1.12 (d, J = 6 Hz, 3H, NCH(C*H*$_3$)$_2$), 1.17 (d, J = 6 Hz, 3H, NCH(C*H*$_3$)$_2$), 1.22 (d, J = 6 Hz, 3H, NCH(C*H*$_3$)$_2$), 1.36 (d, J = 6 Hz, 3H, NCH(C*H*$_3$)$_2$), 1.41 (d, J = 6 Hz, 3H, NCH(C*H*$_3$)$_2$), 1.45 (d, J = 6 Hz, 3H, NCH(C*H*$_3$)$_2$), 1.51 (d, J = 6 Hz, 3H, NCH(C*H*$_3$)$_2$), 2.14 (s, 3H, NArC*H*$_3$), 2.20 (s, 3H, NArC*H*$_3$), 2.27 (s, 6H, NC*H*$_3$), 2.35 (s, 6H, NC*H*$_3$), 3.44 (m, 1H, NC*H*(CH$_3$)$_2$), 3.63 (m, 3H, NC*H*(CH$_3$)$_2$), 7.06 (d, J = 8 Hz, 2H, NA*r*CH$_3$), 7.33 (d, J = 8 Hz, 2H, NA*r*CH$_3$), 7.84 (d, J = 8 Hz, 2H, NA*r*CH$_3$). The fourth aryl doublet is obscured by the solvent peak. ^{13}C{^{1}H}NMR (C$_6$D$_6$, 125 MHz): δ 21.4 (s, NCH(*C*H$_3$)$_2$), 24.1 (s, NCH(*C*H$_3$)$_2$), 24.5 (s, NCH(*C*H$_3$)$_2$), 24.6 (s, NCH(*C*H$_3$)$_2$), 25.1 (s, NCH(*C*H$_3$)$_2$), 25.5 (s, NCH(*C*H$_3$)$_2$), 25.9 (s, NCH(*C*H$_3$)$_2$), 26.0 (s, NCH(*C*H$_3$)$_2$), 39.8 (s, N*C*H$_3$), 39.9 (s, N*C*H$_3$), 49.0 (s, Ar*C*H$_3$), 49.5 (s, Ar*C*H$_3$), 50.8 (s, N*C*H(CH$_3$)$_2$), 51.1 (s, N*C*H(CH$_3$)$_2$), 123.8 (s, Ar), 125.3 (s, Ar), 128.7 (s, Ar), 129.6 (s, Ar), 131.1 (s, Ar), 132.6 (s, Ar), 147.3 (s, NAr), 149.7 (s, NAr), 161.7 (s, S*C*(N^{i}Pr)$_2$), 170.3 (s, N$_3$*C*), 174.4 (s, N$_3$*C*). IR (cm^{-1}): 1555 (s), 1520 (s), 1502 (m), 1401 (s), 1315 (m), 1285 (m), 1229 (m), 1198 (m), 1179 (m), 1134 (m), 1105 (m), 1056 (s), 946 (m), 928 (w), 819 (w), 742 (w). Anal. Calcd for $C_{33}H_{56}N_8STi$: C, 61.47; H, 8.47; N, 17.43. Found: C, 61.57; H, 8.46; N, 17.16.

NMR Scale Reaction of 5 with ^{i}PrNCN ^{i}Pr. Complex **5** (10.0 mg, 0.0119 mmol), diisopropylcarbodiimide (11.5 mg, 0.0911 mmol), and 1,3,5-trimethoxybenzene internal standard (2.0 mg, 0.012 mmol) were weighed into a vial. C$_6$D$_6$ was added to dissolve the solids, and the solution was transferred to an NMR tube. After 2 h at room temperature, the ^{1}H NMR spectrum showed formation of [Me$_2$NC(N^{i}Pr)$_2$]$_2$Ti[SC-(N^{i}Pr)$_2$] (**7**) (99% conversion versus internal standard). ^{1}H NMR (C$_6$D$_6$, 500 MHz): δ 1.02 (d, J = 7 Hz, 3H, NCH(C*H*$_3$)$_2$), 1.25 (d, J = 7 Hz, 3H, NCH(C*H*$_3$)$_2$), 1.29 (d, J = 7 Hz, 3H, NCH(C*H*$_3$)$_2$), 1.37 (d, J = 7 Hz, 3H, NCH(C*H*$_3$)$_2$), 1.43 (d, J = 7 Hz, 3H, NCH(C*H*$_3$)$_2$), 1.49 (m, 12H, NCH(C*H*$_3$)$_2$), 1.60 (d, J = 7 Hz, 3H, NCH(C*H*$_3$)$_2$), 1.77 (d, J = 7 Hz, 3H, NCH(C*H*$_3$)$_2$), 1.82 (d, J = 7 Hz, 3H, NCH(C*H*$_3$)$_2$), 2.33 (s, 6H, NC*H*$_3$), 2.40 (s, 6H, NC*H*$_3$), 3.38 (sept, J = 7 Hz, 2H, NC*H*(CH$_3$)$_2$), 3.70 (m, 4H, NC*H*(CH$_3$)$_2$), 4.41 (sept, J = 7 Hz, 2H, NC*H*(CH$_3$)$_2$), 4.97 (sept, J = 7 Hz, 2H, NC*H*(CH$_3$)$_2$).

{[Me$_2$NC(N^{i}Pr)$_2$]$_2$Ti(S)dmap (8). A solution of 4-(dimethylamino)-pyridine (0.044 g, 0.360 mmol) in 25 mL of toluene was added to {[Me$_2$NC(N^{i}Pr)$_2$]$_2$TiS}$_2$ (0.150 g, 0.178 mmol) in toluene (40 mL), and the mixture was stirred overnight. The volatile materials were removed under reduced pressure, and the solid residue was extracted with diethyl ether (50 mL). The orange−red solution was filtered through a fritted disk with a pad of Celite. The resulting solution was concentrated to 5 mL and cooled to −30 °C. The orange microcrystalline solid was isolated by filtration (0.050 g, 33%). ^{1}H NMR (C$_6$D$_6$, 500 MHz): δ 1.55 (br, 24 H, NCH(C*H*$_3$)$_2$), 2.18 (s, 12H, N$_2$CN(C*H*$_3$)$_2$), 2.51 (br s, 6H, NC$_5$H$_4$−N(C*H*$_3$)$_2$), 3.76 (br, 4H, NC*H*(CH$_3$)$_2$), 6.07 (d, J = 6 Hz, NC$_5$*H*$_4$−N(CH$_3$)$_2$), 8.67 (br, NC$_5$*H*$_4$−N(CH$_3$)$_2$). IR (cm^{-1}): 1613 (s), 1521 (s), 1358 (s), 1313 (m), 1230 (s), 1201(m), 1135 (s), 1118 (s), 1048 (s), 1006 (s), 945 (m), 830 (m), 812 (m), 738 (m). EI−MS (*m*/*z*): 543 (M$^+$) Anal. Calcd for $C_{25}H_{50}N_8STi$: C, 55.32; H, 9.28; N, 20.66. Found: C, 55.60; H, 9.50; N, 20.32.

General Experimental Details for X-ray Structure Determinations. Crystals were mounted onto glass fibers, using Paratone N hydrocarbon oil, and transferred to a Siemens SMART diffractometer/CCD area detector,[50] centered in the beam, and cooled by a nitrogen-flow low-temperature apparatus. Preliminary orientation matrix and cell constants were determined by collection of 60 10 s frames followed by spot integration and least squares refinement. A hemisphere of data was collected using ω scans of 0.3° counted for a total of 10 s per frame. The raw data were integrated by the program SAINT.[51] Data analysis was performed using XPREP.[52] For **3**, an absorption correction was applied using XPREP; for **1**, **2**, and **4**−**6**, the correction was applied using SADABS.[53] The unit cell parameters and statistical analysis of the intensity distribution were used for space group determination.[54] The data were corrected for Lorentz and polarization effects, but no correction for crystal decay was applied. Unique equivalent reflections were merged. The structures were solved by direct methods[55] and expanded using Fourier techniques.[56] Except as noted, all non-hydrogen atoms were refined anisotropically, and hydrogen atoms were included as fixed contributions, but not refined. The quantity minimized by the least-squares program was $\Sigma w(|F_o| - |F_c|)^2$, where w is the weight of a given observation. The weighting scheme was based on counting statistics and included a factor (p = 0.030) to downweight the intense reflections. The analytical forms of the scattering factor tables for the neutral atoms were used,[57] and all scattering factors were corrected for both the real and imaginary components of anomalous dispersion.[58] All calculations were performed using the teXsan[59] crystallographic software package of Molecular Structure Corp.

(50) *SMART*; Area-Detector Software Package, Siemens Industrial Automation, Inc.: Madison, WI, 1995

(51) *SAINT* ; SAX Area-Detector Integration Program (V 4.024); Siemens Industrial Automation, Inc.: Madison, WI, 1995

(52) *XPREP* (V 5.03); Part of the SHELXTL Crystal Structure Determination; Siemens IndustrialAutomation, Inc.: Madison, WI, 1995

(53) SADABS; Siemens Area Detector ABSorption correction program, George Sheldrick, 1996. Advance copy, private communication.

(54) Cromer, D. T.; Waber, J. T. *International Tables for X-ray Crystallography*, Vol. IV; The Kynoch Press: Birmingham, England, 1974; Table 2.2 A.

(55) *SIR92*; Altomare, A., Burla, M. C., Camalli., Cascarano, M., Giacovazzo, C., Guagliardi, A., Polidori, G. 1994.

(56) Beurskens, P. T.; Admiraal, G.; Beurskens, G.; Bosman, W. P.; Garcia-Granda, S.,; Gould, R. O.; Smits, J. M. M.; Smykalla, C. *DIRDIF92*; The DIRDIF program system, Technical Report of the Crystallography Laboratory; University of Nijmegen: The Netherlands,1992.

(57) Creagh, D. C.; Hubbell, J. H. In *International Tables for Crystallography*, Vol C; Wilson, A. J. C., Ed.; Kluwer Academic Publishers: Boston, 1992; Table 4.2.4.3, pp 200−206.

(58) Ibers, J. A.; Hamilton, W. C. *Acta Crystallogr.* **1964**, *17*, 781.

(59) *teXsan*; Crystal Structure Analysis Package, Molecular Structure Corporation, 1985 & 1992.

The carbon atoms of complex **2**, C6, C7, C19, and C20, constitute a disordered isopropyl group; each atom was refined isotropically at half occupancy.

Acknowledgment. We are grateful for financial support of this work from the NSF (Grant No. CHE-9633374 to R.G.B. and CHE-0072819 to J.A.). We wish to acknowledge Dr. R. Nunlist and T. Barnum of the UC Berkeley NMR facility for assistance with low temperature NMR experiments, and Dr. G. Ball of the University of New South Wales for helpful discussions. CNDOS is supported by Bristol−Myers Squibb as a sponsoring member.

Supporting Information Available: Crystallographic data for compounds **1**−**6**, including ORTEP diagrams, tables of crystal data and data collection parameters, atomic coordinates, anisotropic displacement parameters, and all bond lengths and bond angles. This material is available free of charge via the Internet at http://pubs.acs.org.

IC010631+